Cosmological Constraints from Type Ia Supernovae Peculiar Velocity Measurements

C. Gordon, K. Land, and A. Slosar
Oxford Astrophysics, Physics, DWB, Keble Road, Oxford, OX1 3RH, United Kingdom
(Received 16 May 2007; published 20 August 2007)

We detect the correlated peculiar velocities of nearby type Ia supernovae (SNe), while highlighting an error in some of the literature. We find $\sigma_8 = 0.79 \pm 0.22$ from SNe, and examine the potential of this method to constrain cosmological parameters in the future. We demonstrate that a survey of 300 low-z SNe (such as the nearby SNfactory) will underestimate the errors on w by ~35% if the coherent peculiar velocities are not included.

DOI: 10.1103/PhysRevLett.99.081301 PACS numbers: 98.62.Py, 95.36.+x, 97.60.Bw, 98.80.Es

The first compelling evidence that the Universe is undergoing a period of accelerated expansion was provided by observations of Type Ia supernovae (SNe) [1,2]. The data from many current [3–5] and near future [6–9] surveys should eventually constrain the effective dark energy equation of state to better than 10%.

Density inhomogeneities cause the SNe to deviate from the Hubble flow, as gravitational instability leads to matter flowing out of underdensities and into overdensities. These ''peculiar velocities'' (PVs) lead to an increased scatter in the Hubble diagram, of which several studies have been made [10–22]. When combining low and high redshift SNe in order to estimate the properties of the dark energy, the velocity contributions are usually modeled as a Gaussian noise term which is uncorrelated between different SNe. However, as recently emphasized [23], in the limit of low redshift $z \lesssim 0.1$ and large sample size, the correlations between SNe PVs contribute significantly to the overall error budget. In this Letter we investigate the effect of incorporating these correlations using the largest available low-redshift compilation [17].

Peculiar velocity covariance.—The luminosity distance, d_L, to a SN at redshift z, is defined such that $\mathcal{F} = \frac{\mathcal{L}}{4\pi d_L^2}$, where $\mathcal{F}$ is the observed flux and $\mathcal{L}$ is the SN's intrinsic luminosity. Astronomers use magnitudes, which are related to the luminosity distance (in megaparsec) by

$$\mu \equiv m - M = 5\log_{10} d_L + 25, \tag{1}$$

where m and M are the apparent and absolute magnitudes, respectively. In the context of SNe, M is a ''nuisance parameter'' which is degenerate with $\ln(H_0)$ and can be marginalized over. For a Friedmann-Robertson-Walker universe the predicted luminosity distance is given by

$$d_L(z) = (1+z)\int_0^z \frac{dz'}{H(z')} \tag{2}$$

in speed of light units, where H is the Hubble parameter. In the limit of low redshift this reduces to $d_L \approx z/H_0$.

The effect of peculiar velocities leads to a perturbation in the luminosity distance (δd_L) given by [23–27]

$$\frac{\delta d_L}{d_L} = \hat{\mathbf{r}} \cdot \left(\mathbf{v} - \frac{(1+z)^2}{H(z) d_L} [\mathbf{v} - \mathbf{v}_O] \right), \tag{3}$$

where $\mathbf{r}$ is the position of the SN, and $\mathbf{v}_O$ and $\mathbf{v}$ are the peculiar velocites of the observer and SN, respectively. Using the cosmic microwave background dipole we can very accurately correct for $\mathbf{v}_O$. This demonstrates how a SNe survey that measures μ and z can estimate the projected PV field. We now relate this to the cosmology.

The projected velocity correlation function, $\xi(\mathbf{r_i}, \mathbf{r_j}) \equiv \langle (\mathbf{v}(\mathbf{r_i}) \cdot \hat{\mathbf{r}}_\mathbf{i})(\mathbf{v}(\mathbf{r_j}) \cdot \hat{\mathbf{r}}_\mathbf{j}) \rangle$, must be rotationally invariant, and therefore it can be decomposed into parallel and perpendicular components [28–30]:

$$\xi(\mathbf{r_i}, \mathbf{r_j}) = \sin\theta_i \sin\theta_j \xi_\perp(r, z_i, z_j) + \cos\theta_i \cos\theta_j \xi_\parallel(r, z_i, z_j),$$

where $\mathbf{r_{ij}} \equiv \mathbf{r_i} - \mathbf{r_j}$, $r = |\mathbf{r_{ij}}|$, $\cos\theta_i \equiv \hat{\mathbf{r}}_\mathbf{i} \cdot \hat{\mathbf{r}}_\mathbf{ij}$, and $\cos\theta_j \equiv \hat{\mathbf{r}}_\mathbf{j} \cdot \hat{\mathbf{r}}_\mathbf{ij}$. In linear theory, these are given by [28–30]

$$\xi_{\parallel,\perp} = D'(z_i) D'(z_j) \int_0^\infty \frac{dk}{2\pi^2} P(k) K_{\parallel,\perp}(kr), \tag{4}$$

where for an arbitrary variable x, $K_\parallel(x) \equiv j_0(x) - \frac{2j_1(x)}{x}$, $K_\perp(x) \equiv j_1(x)/x$. $D(z)$ is the growth function, and derivatives are with respect to conformal time. $P(k)$ is the matter power spectrum. This corrects the formulas used in [31,32]; see the Appendix for details.

The above estimate of $\xi(\mathbf{r_i}, \mathbf{r_j})$ is based on linear theory. On scales smaller than about $10h^{-1}$ Mpc nonlinear contributions become important. These are usually modeled as an uncorrelated term which is independent of redshift, often set to $\sigma_v \sim 300$ km/s. Comparison with numerical simulations [33] has confirmed that this is an effective way of accounting for the nonlinearities. Other random errors that are usually considered are those from the light curve fitting ($\mu_{\rm err}$), and intrinsic magnitude scatter (σ_m) found to be ~0.08 in the case of [17].

In Fig. 1 we compare the covariance of $\delta d_L/d_L$ from peculiar velocities for a pair of SN

$$C_v(i,j) = \left(1 - \frac{(1+z)^2}{H d_L}\right)_i \left(1 - \frac{(1+z)^2}{H d_L}\right)_j \xi(\mathbf{r_i}, \mathbf{r_j}) \tag{5}$$

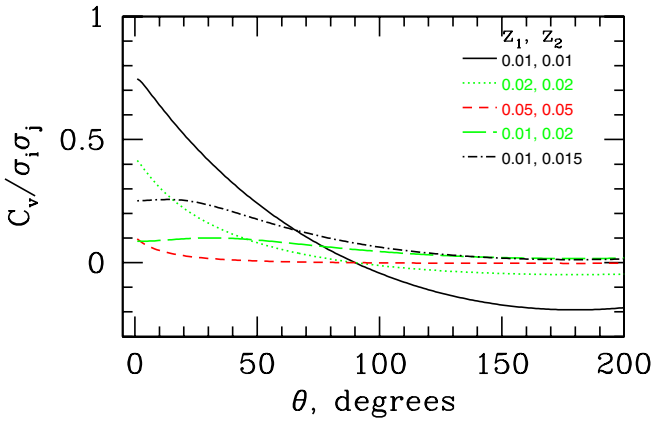

FIG. 1 (color online). The ratio of the covariance from peculiar velocities C_v, compared to the random errors σ, for a pair of supernovae, over a range of angular separations, θ.

to the standard uncorrelated random errors given by

$$\sigma(i)^2 = \left(\frac{\ln(10)}{5}\right)^2[\sigma_m^2 + \mu_{\rm err}(i)^2] + \left(1 - \frac{(1+z)^2}{Hd_L}\right)_i^2 \sigma_v^2 \tag{6}$$

with $\{\Omega_m, \Omega_b, h, n_s, w, \sigma_8\} = \{0.3, 0.05, 0.7, 0.96, -1, 0.85\}$ and $\{\mu_{\rm err}, \sigma_m, \sigma_v\} = \{0.1, 0.08, 300\}$. We see that the PV covariance is comparable with the uncorrelated errors for low z, and we note that the correlated errors become more significant the larger the data set.

Constraints from current data.—An uncorrelated-error-only analysis of SNe allows one to constrain the cosmological parameters through the Hubble parameter in (2). Namely, Ω_m and w, for a flat universe. However, by fitting for the PV covariance we probe the matter power spectrum and can therefore constrain further parameters such as Ω_b, H_0, n_s, σ_8, where these have their usual meaning. In the following analysis we also allow the SNe "nuisance" parameters M, σ_m, σ_v to vary. These are often set to fixed values; however, marginalizing over them allows a better estimate of the uncertainty in the other parameters. The weighted integration of the matter power spectrum in Eq. (4) has similar weights to those used in evaluating σ_8. Therefore, the higher σ_8, the stronger the correlations between the projected velocities, obeying $C_v \propto \sigma_8^2$ for the other parameters fixed.

We analyze nearby supernovae ($z \leq 0.12$) from [17], who find improved luminosity distances to 133 supernovae from a multicolor light curve method. Following [17], we exclude 9 supernovae from the set. These are supernovae that are unsuitable due to bad light curve fits, those who have their first observation more than 20 days after maximum light, are hosted in galaxies with excessive extinction ($A_V^0 > 2.0$ mag) and one outlier (SN1999e). This leaves 124 supernovae $z \in [0.0023, 0.12]$, which have an average separation of $\bar{r} = 108h^{-1}$ Mpc, a mean redshift $\bar{z} = 0.024$, and herein we refer to this data set as our "low-z" SNe.

The likelihood is given by $\mathcal{L} \propto |\Sigma|^{-1/2} e^{-(1/2)x^T\Sigma^{-1}x}$, where $\Sigma(i,j) = C_v(i,j) + \sigma(i)^2\delta_{ij}$ and $x = [d_L^{\rm obs} - d_L(z)]/d_L(z)$ with $d_L^{\rm obs}$ given by Eq. (1), and $d_L(z)$ by Eq. (2). We assume a flat universe with a cosmological constant ($w = -1$), a big bang nucleosynthesis (BBN) prior $\Omega_b h^2 \sim \mathcal{N}(0.0214, 0.002)$ [34], and a Hubble Space Telescope (HST) prior $h \sim \mathcal{N}(0.72, 0.08)$ [35]. These two priors remove models that are wildly at odds with standard cosmological probes, but do not unduly bias results towards standard cosmology. The likelihood has almost negligible dependence on n_s, and to keep it in a range consistent with CMB and large scale structure estimates we give it a uniform prior $n \in [-0.9, 1.1]$. The other parameters are all given broad uniform priors. We use the standard Markov Chain Monte Carlo (MCMC) method to generate samples from the posterior distribution of the parameters [36].

The low-z results are given in row A of Table I. As a nonzero σ_8 is needed for the velocity correlations, these results indicate the correlations are detected at the 3.6σ level. We also perform the MCMC calculations without including the PV covariance matrix C_v, and we find $-2\ln\mathcal{L}_{\rm max}$ increases by 19.3. As the likelihood no longer depends on $\{\sigma_8, \Omega_b, h, n_s\}$, we have removed four parameters.

When estimating the cosmological parameters from SNe, a low-redshift cut is usually imposed, to reduce the effects of the PVs. For example, in [37], their SNe data set has 192 SNe with $z \in [0.016, 1.76]$ and a mean redshift of $\bar{z} = 0.48$. Herein we refer to this data set as our "high-z" SNe. Our MCMC results for just this data (without including PVs) are shown in row B of Table I. Although we marginalize over the SNe parameters $\{M, \sigma_v, \sigma_s\}$, our constraints on Ω_m are still in excellent agreement with those obtained in [37].

We now combine the low-z and the high-z data sets, to make an "all-z" data set. We used the overlapping SNe in the two data sets to estimate a small normalizing offset to the magnitudes from the latter data set, (the extra magnitude error is negligibly small). The same procedure was used by [37] in constructing their data set. After eliminating duplicated SNe, our combined all-z data set has 271 SNe with $z \in [0.0023, 1.76]$, and $\bar{z} = 0.35$. Our all-z results are given in row C of Table I. The constraints on σ_8 broaden slightly due to a mild degeneracy between σ_8 and Ω_m, which is broken by the addition of the higher z SNe, but pushes σ_8 to the region of higher uncertainty.

Because of a degeneracy between w and Ω_m, it is necessary to combine the SNe with another data source. Here we use the Wilkinson Microwave Anisotropy Probe (WMAP) CMB data [38]. We continue to assume a flat universe, and we now allow w to be a free parameter. The results are given in rows D to H of Table I and in Fig. 2. As can be seen by comparing rows D and E, if a redshift cutoff of $z \geq 0.016$ is made, then current data has a systematic error of $\delta w = 0.02$ when PVs are not included. This is several times smaller than the statistical error of $\delta w = 0.08$. However, comparing rows F and G, shows that if no

TABLE I. Mean and 68% confidence limits on the cosmological parameters, and σ_v, σ_m, using different combinations of the WMAP and SNe data sets, with and without including the peculiar velocity covariance matrix. See text for discussion.

	w	σ_8	Ω_m	σ_v	σ_m
(A) low-z + PV + BBN + HST	-1	$0.79^{+0.22}_{-0.22}$	$0.48^{+0.30}_{-0.29}$	275^{+69}_{-70}	$0.08^{+0.03}_{-0.04}$
(B) high-z	-1		$0.27^{+0.03}_{-0.03}$	363^{+169}_{-185}	$0.12^{+0.02}_{-0.02}$
(C) all-z + PV + BBN + HST	-1	$0.78^{+0.23}_{-0.23}$	$0.30^{+0.04}_{-0.04}$	$301^{+53.9}_{-53.4}$	$0.1^{+0.02}_{-0.02}$
(D) high-z + WMAP	$-0.96^{+0.09}_{-0.09}$	$0.76^{+0.07}_{-0.07}$	$0.26^{+0.03}_{-0.03}$	191^{+97}_{-104}	$0.10^{+0.02}_{-0.02}$
(E) high-z + PV + WMAP	$-0.94^{+0.08}_{-0.08}$	$0.75^{+0.06}_{-0.06}$	$0.26^{+0.02}_{-0.03}$	149^{+107}_{-108}	$0.11^{+0.02}_{-0.02}$
(F) all-z + WMAP	$-0.93^{+0.07}_{-0.07}$	$0.75^{+0.06}_{-0.07}$	$0.26^{+0.02}_{-0.02}$	395^{+42}_{-42}	$0.11^{+0.02}_{-0.02}$
(G) all-z + PV + WMAP	$-0.86^{+0.08}_{-0.08}$	$0.72^{+0.06}_{-0.07}$	$0.28^{+0.03}_{-0.03}$	292^{+44}_{-45}	$0.11^{+0.02}_{-0.02}$
(H) WMAP only	$-0.99^{+0.22}_{-0.22}$	$0.76^{+0.09}_{-0.09}$	$0.25^{+0.05}_{-0.05}$		

redshift cutoff is made, neglecting the correlated PVs results in a systematic error of $\delta w = 0.07$ which is about as large as the statistical error.

An alternative approach of accounting for the correlated peculiar velocities is to estimate the underlying density field from galaxy redshift surveys and then use this to try and remove peculiar velocity at each SNe [21]. As this method has different systematics to the statistical modeling method we have investigated, we believe it will be a useful cross check to apply both methods to future SNe data sets and compare the results.

Forecasts.—We now consider the relevance of peculiar velocities to future supernovae surveys, using a Fisher matrix analysis. The Fisher (information) matrix probes the ability of an experiment to constrain parameters, by looking at the dependence of the likelihood $F_{\alpha\beta} \equiv -\langle \frac{\partial^2 \ln \mathcal{L}}{\partial p_\alpha \partial p_\beta} \rangle$,

$$F_{\alpha\beta} = \mathbf{d}_{,\alpha}\, C^{-1} \mathbf{d}^T{}_{,\beta} + \tfrac{1}{2} \mathrm{Tr}(C^{-1} C_{,\alpha}\, C^{-1} C_{,\beta}). \quad (7)$$

Often the second term is ignored; however, we find that this approximation is no longer valid when including PVs. Unmarginalized 1σ errors on parameter p_α are given by $\sqrt{(1/F_{\alpha\alpha})}$, and the equivalent marginalized errors by $\sqrt{(\{F^{-1}\}_{\alpha\alpha})}$. Generally, the inverted Fisher matrix F^{-1} provides the expected covariance matrix for the parameters.

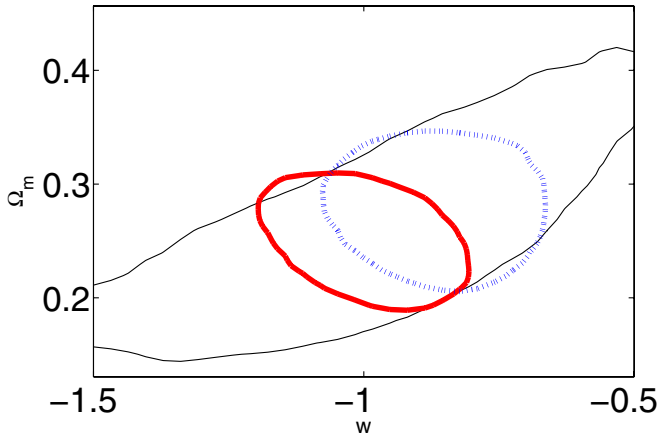

FIG. 2 (color online). 95% confidence limits on Ω_m and w, for WMAP only (thin black lines), WMAP with high-z SNe (thick red line), and WMAP with all-z SNe including PVs (dotted blue line).

We consider two future supernovae experiments that aim to detect high and low-redshift supernovae, respectively: the Supernova/Acceleration Probe (SNAP, [9]), and the Nearby Supernova Factory (SNfactory, [6]). The baseline SNfactory program is to obtain spectrophotometric light-curves for SNe in the redshift range $0.03 < z < 0.08$, with the assumption that these SNe are far enough away for correlated peculiar velocities to not contribute significantly to the error budget. However, in Fig. 1 we can see the contribution of correlated PVs is not irrelevant for $z \sim 0.03$, and as the number of SNe increases the overall uncertainty from random errors (such as intrinsic magnitude scattter and instrumental noise) gets beaten down by a $1/\sqrt{N}$ factor, while the correlated errors from coherent peculiar velocities do not. Thus at any redshift, these peculiar velocity errors will begin to dominate for some large number of SNe. We investigate the situation for the SNfactory by considering 300 SNe randomly distributed over a rectangular area of 10 000 sq degrees, and redshifts $0.03 < z < 0.08$. We also include high-z from a SNAP-like survey, and model this as 2000 SNe randomly distributed over 10 sq degrees with $0.2 < z < 1.7$, and we assume PVs are irrelevant for these SNe. We take our fiducial model to be a flat ΛCDM cosmology with $\Omega_m = 0.3$, $\Omega_b = 0.05$, $h = 0.7$, $n_s = 0.96$, $w = -1$, $\sigma_8 = 0.85$, and nuisance parameters $\sigma_v = 300$ km/s, $\sigma_m = 0.1$, $\mu_{\mathrm{err}} = 0.1$. We further marginalize over M.

As can be seen from Fig. 3, the contours increase significantly when low-z SNe are not available (marginalized error on w increase to 0.12), even when CMB data is included. In Fig. 3 we also compare the marginalized 1σ contours obtained when the coherent PVs are ignored and included, for our hypothetical SNAP and SNfactory surveys. We see that, even for a cut of $z > 0.03$ the error bars on Ω_m and w will be considerably underestimated if the peculiar velocities are ignored, and, in particular, the marginalized error on w increases by 35% from 0.062 to 0.084, for the SNe alone. We therefore conclude that it is

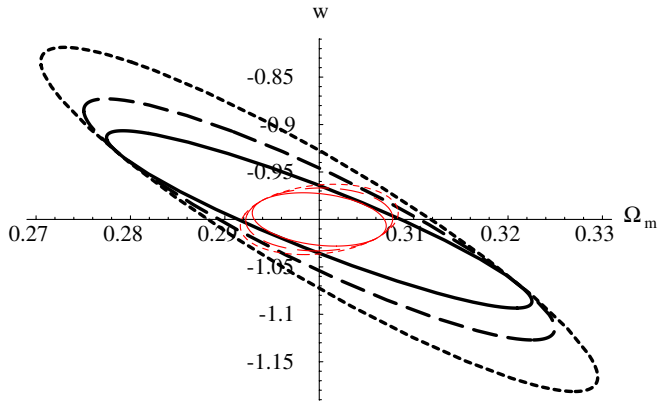

FIG. 3 (color online). The marginalized 1σ contours for Ω_m and w from a SNAP-like high-z SNe survey in a flat ΛCDM cosmology (short dashed lines). We also consider including 300 low-z SNe from a SNfactorylike survey, while ignoring peculiar velocities (solid lines) and including them (long dashed lines). Smaller red contours include cosmic variance limited CMB, up to $\ell = 2000$.

essential to include a full covariance matrix analysis at these redshifts, to avoid significantly underestimating the errors. That the error bars increase rather than decrease indicates that the extra information available in the peculiar velocities is outweighed by the extra parameter space $\{\Omega_b, h, n_s, \sigma_8\}$.

We thank Joe Silk, Pedro Ferreira, and Uroš Seljak for useful conversations. C. G. is funded by the Beecroft Institute for Particle Astrophysics and Cosmology, K. R. L. by Glasstone and Christ Church college, A. S. by Oxford Astrophysics. Results were computed on the UK-CCC COSMOS supercomputer.

Appendix.—For perturbations, $\rho(1+\delta)$, and peculiar velocity $\mathbf{v}$ we find the perturbed Fourier space continuity equation, in comoving coordinates, is $\delta'_{\mathbf{k}} - i\mathbf{k}\cdot\mathbf{v}_{\mathbf{k}} = 0$, where prime indicates differentiation with respect to conformal time, η. Using the linear approximation $\delta_{\mathbf{k}}(\eta) = D(\eta)\tilde{\delta}_{\mathbf{k}}$, and assuming that the universe has no vorticity ($\nabla \times \mathbf{v} = 0$) leads to $\mathbf{v}_{\mathbf{k}} = -iD'\frac{\tilde{\delta}_{\mathbf{k}}}{k^2}\mathbf{k}$, where $D(z)$ is the growth function. Therefore, the Fourier space correlation between the ith component of the velocity field at time η_A and the jth component of the velocity field at time η_B is given by

$$\langle v^i_{\mathbf{k_A}} v^{j*}_{\mathbf{k_B}} \rangle = D'(\eta_A)D'(\eta_B)(2\pi)^3\delta(\mathbf{k_A} - \mathbf{k_B})P(k_A)\frac{k^i_A k^j_A}{(k_A)^4},$$

where $\langle \delta_{\mathbf{k_A}} \delta_{\mathbf{k_B}} \rangle = (2\pi)^3\delta(\mathbf{k_A} - \mathbf{k_B})P(k_A)$, and the subscripts denote the quantity at time η_A or η_B. This corrects equation (B1) of [31], and our resulting Eq. (5) for C_v corrects those of [32], among others.

[1] A. G. Riess *et al.* (Supernova Search Team), Astron. J. **116**, 1009 (1998).
[2] S. Perlmutter *et al.* (Supernova Cosmology Project), Astrophys. J. **517**, 565 (1999).
[3] P. Astier *et al.*, Astron. Astrophys. **447**, 31 (2006).
[4] A. G. Riess *et al.*, Astrophys. J. **659**, 98 (2007).
[5] W. M. Wood-Vasey *et al.*, arXiv:astro-ph/0701041.
[6] G. Aldering *et al.*, in *Survey and Other Telescope Technologies and Discoveries*, edited by J. A. Tyson and S. Wolff (SPIE, 2002), Vol. 4836, p. 61.
[7] B. Dilday *et al.*, Bull. Am. Astron. Soc. 37, 1459 (2005).
[8] M. Hamuy *et al.*, arXiv:astro-ph/0512039.
[9] G. Aldering, New Astron. Rev. **49**, 346 (2005).
[10] A. G. Riess, W. H. Press, and R. P. Kirshner, Astrophys. J. **445**, L91 (1995).
[11] A. G. Riess, M. Davis, J. Baker, and R. P. Kirshner, arXiv:astro-ph/9707261.
[12] I. Zehavi, A. G. Riess, R. P. Kirshner, and A. Dekel, Astrophys. J. **503**, 483 (1998).
[13] A. Bonacic, R. A. Schommer, N. B. Suntzeff, and M. M. Phillips, Bull. Am. Astron. Soc. **32**, 1285 (2000).
[14] D. J. Radburn-Smith, J. R. Lucey, and M. J. Hudson, arXiv:astro-ph/0409551.
[15] C. Bonvin, R. Durrer, and M. Kunz, Phys. Rev. Lett. **96**, 191302 (2006).
[16] T. Haugboelle *et al.*, arXiv:astro-ph/0612137.
[17] S. Jha, A. G. Riess, and R. P. Kirshner, Astrophys. J. **659**, 122 (2007).
[18] R. Watkins and H. A. Feldman, Mon. Not. R. Astron. Soc. **379**, 343 (2007).
[19] A. Conley *et al.*, Astrophys. J. Lett. **664**, L13 (2007).
[20] L. Wang, arXiv:astro-ph/0705.0368.
[21] J. D. Neill, M. J. Hudson, and A. Conley, Astrophys. J. Lett. **661**, L123 (2007).
[22] S. Hannestad, T. Haugboelle, and B. Thomsen, arXiv:astro-ph/0705.0979.
[23] L. Hui and P. B. Greene, Phys. Rev. D **73**, 123526 (2006).
[24] M. Sasaki, Mon. Not. R. Astron. Soc. **228**, 653 (1987).
[25] N. Sugiura, N. Sugiyama, and M. Sasaki, Prog. Theor. Phys. **101**, 903 (1999).
[26] T. Pyne and M. Birkinshaw, Mon. Not. R. Astron. Soc. **348**, 581 (2004).
[27] C. Bonvin, R. Durrer, and M. A. Gasparini, Phys. Rev. D **73**, 023523 (2006).
[28] K. Gorski, Astrophys. J. **332**, L7 (1988).
[29] E. J. Groth, R. Juszkiewicz, and J. P. Ostriker, Astrophys. J. **346**, 558 (1989).
[30] S. Dodelson, *Modern Cosmology* (Academic, New York, 2003).
[31] C. Hernandez-Monteagudo, L. Verde, R. Jimenez, and D. N. Spergel, Astrophys. J. **643**, 598 (2006).
[32] A. Cooray and R. R. Caldwell, Phys. Rev. D **73**, 103002 (2006).
[33] L. Silberman, A. Dekel, A. Eldar, and I. Zehavi, Astrophys. J. **557**, 102 (2001).
[34] D. Kirkman, D. Tytler, N. Suzuki, J. M. O'Meara, and D. Lubin, Astrophys. J. Suppl. Ser. **149**, 1 (2003).
[35] W. L. Freedman *et al.*, Astrophys. J. **553**, 47 (2001).
[36] A. Lewis and S. Bridle, Phys. Rev. D **66**, 103511 (2002).
[37] T. M. Davis *et al.*, arXiv:astro-ph/0701510.
[38] D. N. Spergel *et al.* (WMAP), Astrophys. J. Suppl. Ser. **170**, 377 (2007).